

# Discovering the Mysteries of Chemical Reactions

*This report features the work of Shih-Huang Lee and his co-workers published in J. Chem. Phys. **141**, 124314 and 194305 (2014); and the work of Laurie J. Butler and his co-workers published in J. Phys. Chem. A **118**, 3211 and 4707 (2014).*

Dudley R. Herschbach, Yuan T. Lee and John C. Polanyi were jointly awarded, in 1986, the Nobel prize in chemistry for their major contributions to chemical dynamics. Among them, Herschbach and Lee studied the detailed internal energies and kinetic energies of products formed from a single collision of two molecules (or radicals). Applying differential pumping and a crossed molecular beam, they built an environment for a reaction involving a single collision with a satisfactory ratio of signal to noise, and opened a window to observe

experimentally the progress of a chemical reaction. Several machines for crossed molecular beams are now distributed world-wide, designed for important chemical reactions and dynamics; one of these is located at the TLS in the NSRRC. This machine is also the only one to take advantage of synchrotron radiation as the source of vacuum-ultraviolet light to ionize products.

Shih-Huang Lee is interested in the interstellar formation of hydrocarbons. He takes advantage of the

crossed-molecular-beam machine coupled with synchrotron radiation at BL21A1 to investigate intensively the reaction mechanisms. Not only atomic carbon and small carbon clusters— $C_2$ ,  $C_3$  and  $C_5$ —but also polyynic radicals, such as  $C_2H$ ,  $C_4H$ ,  $C_6H$  and  $C_8H$ , were detected in hydrocarbon-rich interstellar and circumstellar environments. Tricarbon,  $C_3$ , has a singlet electronic ground state,  $^1C_3$ , and triplet first excited state,  $^3C_3$ . Because its reactions have large barriers,  $^1C_3$  has typically little reactivity with unsaturated hydrocarbons; no work on highly reactive  $^3C_3$  has been performed. Lee mixed  $C_4F_6$  and He to generate  $^3C_3$  in the molecular beam with an electric discharge. Varying the photon energy of a tunable source of vacuum-ultraviolet light, he found a method to form a small amount of  $^3C_3$  radical.<sup>1</sup> Figure 1 shows the photoionization spectrum of  $C_3$  radicals. The ionization energy is 10 eV for  $^3C_3$  and 11.6 eV for  $^1C_3$ . Although a dominant signal from  $C_3$  radical has an onset at 11.6 eV, he measured a small signal from 10 eV, assigned to  $^3C_3$ . He designed the experiments with a small collision energy so that  $^1C_3$  radical was unable to react because the total energy was inadequate to overcome the reaction barrier. In that environment of a reactant with a background free of interference, the measured products were expected to be produced from only  $^3C_3$ .

Besides the possible background from reactants, some product signal might also arise from the background. Among several parameters to decrease the incorrect signal, the first is to ensure the scattering directions of products. Figure 2 shows a Newton diagram of the reaction  $^3C_3 + C_2H_2 \rightarrow C_5H + H$ . In this experiment, the velocities of  $^3C_3$  and  $C_2H_2$  were fixed; the velocity of the center of mass was thus well defined as  $V_{rel}$ . According to a calculation of the possible kinetic energies, product  $C_5H$  was detectable only between  $24^\circ$  and  $48^\circ$ .

The signal of the corresponding duration of flight for product  $C_5H$  to arrive at the detector at each scattering angle is displayed in Figure 3. The signal observed at angles larger than  $48^\circ$  and less than  $24^\circ$  was defined as

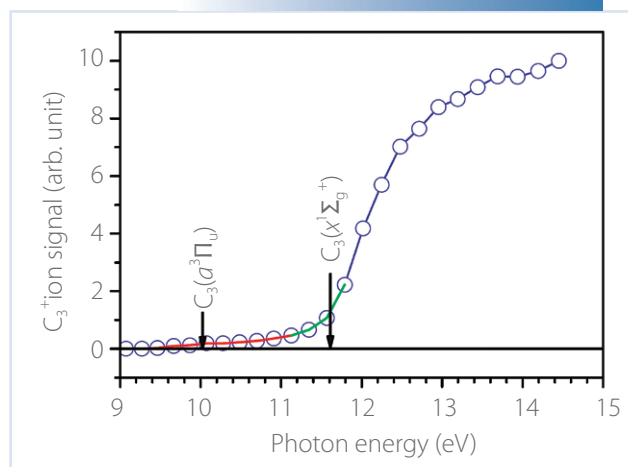


Fig. 1: Photoionization spectrum of reactant  $C_3$ . Arrows indicate deconvoluted ionization thresholds  $10.0 \pm 0.2$  eV of  $^3C_3$  and  $11.6 \pm 0.2$  eV of  $^1C_3$ . Red and green lines serve as visual guides to the thresholds of  $^3C_3$  and  $^1C_3$ , respectively. (Reproduced from Ref. 1)

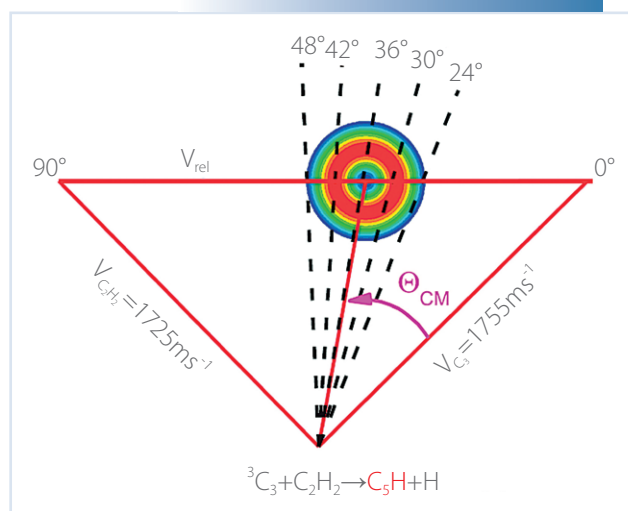
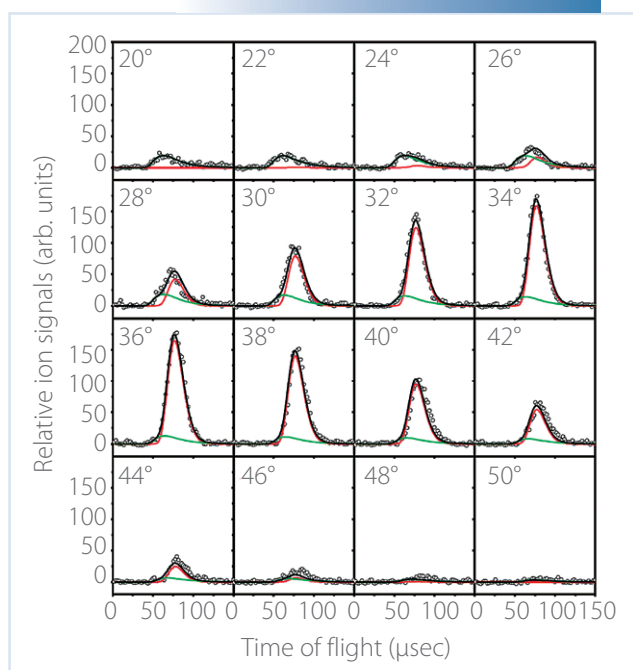
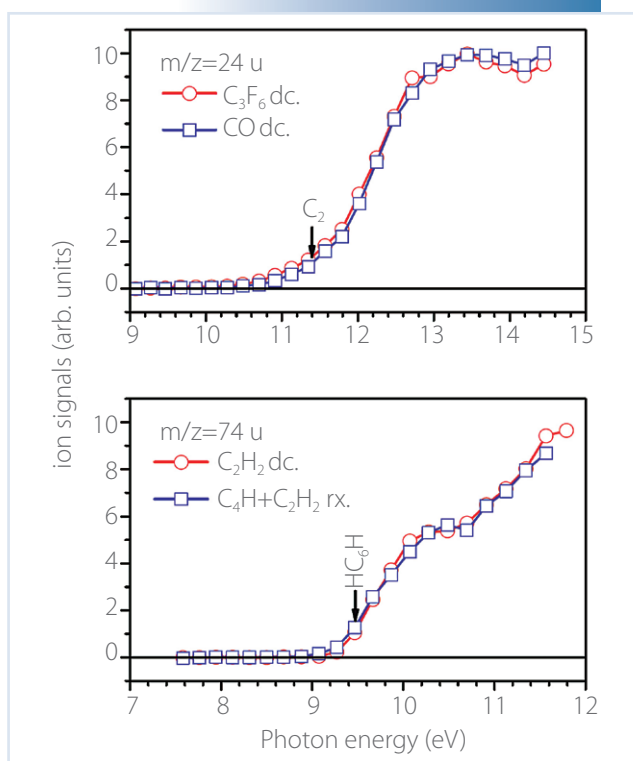


Fig. 2: Newton diagram superimposed on a two-dimensional map of the velocity distribution of product  $C_5H$  from reaction  $^3C_3 + C_2H_2 \rightarrow C_5H + H$ .  $V_{C_3}$  ( $V_{C_2H_2}$ ) denotes the velocity of reactant  $C_3$  ( $C_2H_2$ ) and  $V_{rel}$  denotes the relative velocity between both reactants. (Reproduced from Ref. 1)

a background effect that might arise from discharging the precursor. Another parameter such as the photon energy of the ionization source was finely tuned for an optimal ratio of signal to noise. The signal from reaction and background were eventually all clearly simulated, as in Fig. 3. On varying the ionization energy, the photoionization spectrum of  $C_5H$  became available to derive the structure of this product. This experiment enabled reactants, products, scattering angle, product structures, and internal energies to be characterized clearly. Coordi-



**Fig. 3:** Angle-specific time-of-flight spectra of product  $C_3H$  from  ${}^3C_3 + C_2H_2$  recorded at  $m/z = 61$  u and photoionization energy 11.6 eV. Circles denote the experimental data and curves denote the simulations. (Reproduced from Ref. 1)



**Fig. 4:** Photoionization spectra of reactants  $C_2$  (upper) and  $C_6H_2$  (lower) produced from 1%  $C_3F_6/He$  and 5%  $C_2H_2/He$ , respectively, in an electric discharge. The photoionization spectrum of  $C_2$  produced from the discharge of 10%  $CO/He$  is shown also in the upper panel. The photoionization spectrum of  $HCC_6H$  produced from the  $C_4H + C_2H_2$  reaction is shown also in the lower panel. (Reproduced from Ref. 2)

nated with theoretical calculations, the surface of potential energy and the extremely rapid events during the reaction were deduced.

Another experiment was performed to shed light on the formation of octatetrayl ( $C_8H$ ).<sup>2</sup> Reactants  $C_2$  and  $C_6H_2$  were generated on discharging precursors in their nozzles. A similar method was adopted to test the properties of the reactants, shown in Fig. 4. The photoionization spectra of reactants  $C_2$  and  $C_6H_2$  are almost identical to those generated with another well-known method; this property was verifiable only with a tunable ionization energy.

The rates of chemical reaction are a major topic of research in atmospheric and combustion chemistry. The rates of those reactions represent statistical results of many collisions with diverse kinetic and internal energies. Secondary reactions are also typically involved. The experimental results vary because they are influenced by many factors. Detailed experiments of chemical dynamics must generally be performed to understand what really happens during the reaction and what influences the reaction rates. Laurie. J. Butler tried to study the addition of OH to propene on generating the radical intermediates formed upon addition of the hydroxyl radical by photodissociation of 1-bromo-2-propanol and 2-bromo-1-propanol. Most experiments were completed on their home-built machine for velocity map ion imaging coupled with resonance-enhanced multiphoton ionization. A problem arose that, if the kinetic energy is small, the signal on the image becomes near the position at which the unreacted ones are located and dominantly buried. A scattering apparatus has this advantage; a minor dissociation channel that was measured is shown in the inset of Fig. 5. The best measurement was deduced on varying the photon energy.<sup>3</sup>

The decomposition paths of energetic materials are complicated but important; both experimental and

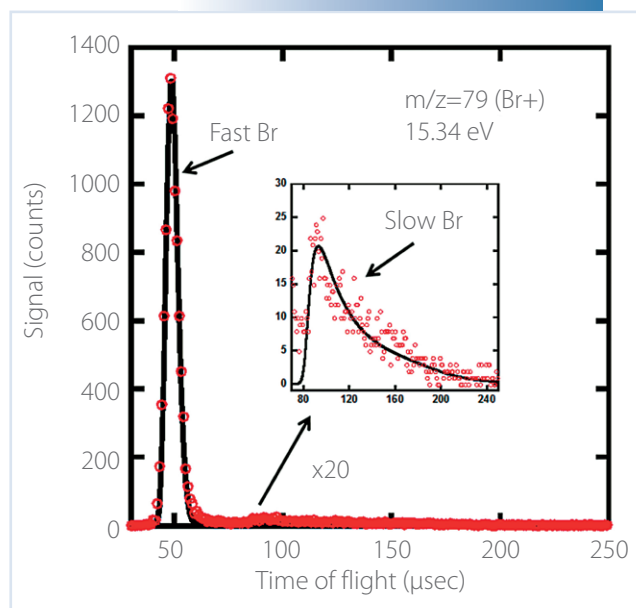


Fig. 5: Time-of-flight spectrum for fragments with  $m/z = 79$  u photochemically dissociated from  $C_3H_6OHBr$ . (Reproduced from Ref. 3)

theoretical research has been undertaken to study this topic but the paths are still unclear. These materials generally pass through nitroalkyl radical or nitroalkene intermediates to their final products. To study the reaction mechanisms of these major intermediate radicals, Butler produced them from the photochemical dissociation of the appropriate halogenated precursors. Although halonitroalkanes would serve as effective precursors for nitroalkyl radicals, their photodissociation dynamics of halonitroalkanes at 193 nm are complicated because of many competing channels of dissociation. In 2013 she found four major channels of dissociation of 2-bromo-2-nitropropane; she used the crossed-molecular-beam machine coupling with tunable VUV light for a detailed clarification. Their paper states “they give extremely detailed information about the photodissociation of halonitroalkanes, which are important to benchmark future photolytic experiments and high-level electronic structure calculations on such molecules.”<sup>4</sup> Figure 6 shows one example. The upper plot presents results using ionization by electron bombardment at energy 200 eV and the lower one is at 10.84 eV. The green line in the lower panel is the new observation of  $NO_2$  products capable of possessing enough vibrational energy to undergo secondary disso-

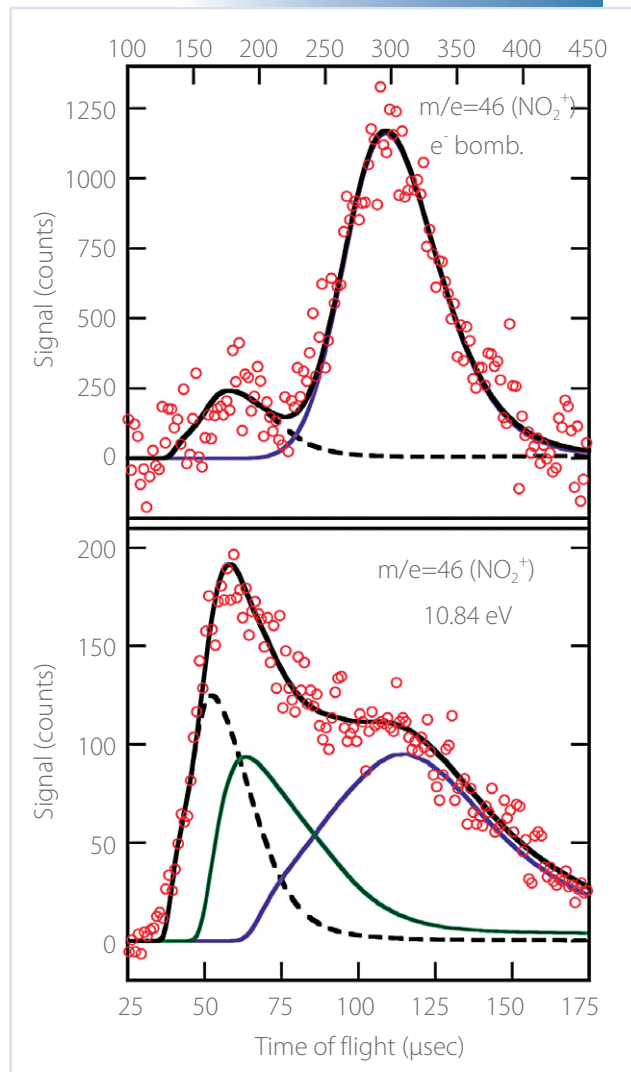


Fig. 6: Time-of-flight spectrum taken at  $m/z = 46$  u, for  $NO_2^+$ , using two methods of detection. Upper frame: acquired at source angle  $10^\circ$  using electron-bombardment ionization at 200 eV. Lower frame: acquired at source angle  $10^\circ$  and photoionization energy 10.84 eV. (Reproduced from Ref. 4)

ciation. During this experiment performed at the TLS, the detailed mechanisms that were resolved could well be applicable to complicated reaction systems.

## References

1. W.-J. Huang, Y.-L. Sun, C.-H. Chin, and S.-H. Lee, *J. Chem. Phys.* **141**, 124314 (2014).
2. Y.-L. Sun, W.-J. Huang, C.-H. Chin, and S.-H. Lee, *J. Chem. Phys.* **141**, 194305 (2014).
3. M. Brynteson, C. C. Womack, R. Booth, S.-H. Lee, J. J. Lin, and L. J. Butler, *J. Phys. Chem. A* **118**, 3211 (2014).
4. R. Booth, M. Brynteson, S.-H. Lee, J. J. Lin, and L. J. Butler, *J. Phys. Chem. A* **118**, 4707 (2014).